A Consensus Tetrapeptide Selected by Phage Display Adopts the Conformation of a Dominant Discontinuous Epitope of a Monoclonal Anti-VWF Antibody That Inhibits the von Willebrand Factor-Collagen Interaction*

Karen Vanhoorelbeke‡, Hilde Depraetere‡, Roland A. P. Romijn§, Eric G. Huizinga§¶, Marc De Maeyer‖, and Hans Deckmyn‡**

From the ‡Laboratory for Thrombosis Research, IRC, KU Leuven Campus Kortrijk, E. Sabbelaan 53, 8500 Kortrijk, Belgium, the §Thrombosis and Haemostasis Laboratory, Department of Haematology, University Medical Center, HP G03.647, P.O. Box 85500, 3508 GA Utrecht, The Netherlands and the ‖Laboratory for Bio-Molecular Modelling KU Leuven Campus Heverlee, Celestijnenlaan 200D, 3001 Heverlee, Belgium

Monoclonal antibody (mAb) 82D6A3 is an anti-von Willebrand factor (VWF) mAb directed against the A3-domain of VWF that inhibits the VWF binding to fibrillar collagens type I and III *in vitro* and *in vivo*. To identify the discontinuous epitope of this mAb, we used phage display, mutant analysis, and peptide modeling. All 82D6A3-binding phages displayed peptides containing the consensus sequence SPWR that could be aligned with P981W982 in the VWF A3-domain. Next, the binding of mAb 82D6A3 to 27 Ala mutants with mutations in the A3-domain of VWF revealed that amino acids Arg[963], Pro[981], Asp[1009], Arg[1016], Ser[1020], Met[1022], and His[1023] are part of the epitope of mAb 82D6A3. Inspection of residues Ser[1020], Arg[1016], Pro[981], and Trp[982] in the three-dimensional structure of the A3-domain demonstrated that these residues are close together in space, pointing out that the structure of the SPWR consensus sequence might mimic this discontinuous epitope. Modeling of a cyclic 6-mer peptide containing the consensus sequence and superposition of its three-dimensional structure onto the VWF A3-domain demonstrated that the Ser and Arg in the peptide matched the Ser[1020] and Arg[1016] in the A3-domain. The Pro residue of the peptide served as a spacer, and the side chain of the Trp pointed in the direction of Trp[982]. In conclusion, to our knowledge, this is the first report where a modeled peptide containing a consensus sequence could be fitted onto the three-dimensional structure of the antigen, indicating that it might adopt the conformation of the discontinuous epitope.

Platelet adhesion to subendothelial structures, more specifically to the thrombogenic compound collagen, is one of the first steps in a sequence of reactions that can lead to arterial thrombosis. Platelets interact with collagen both in a direct manner via their collagen receptors (*e.g.* $\alpha_2\beta_1$ (1, 2) and glycoproteins IV

(3) and VI (4, 5)) and indirectly with VWF,[1] forming the bridge between collagen and its platelet receptor glycoprotein Ib/IX/V (6). Binding via both $\alpha_2\beta_1$ and VWF is necessary to sustain platelet adhesion under high shear forces (7–9); VWF-mediated interaction results in rolling of the platelets over the collagen surface (10), upon which the collagen receptors can interact with the damaged vessel wall, leading to firm adhesion. This is the result of platelet activation by the signal-transducing glycoprotein VI (11), leading to a gain-in-affinity of $\alpha_2\beta_1$ (12) and activation of $\alpha_{IIb}\beta_3$ with platelet aggregation as a consequence.

Both $\alpha_2\beta_1$ and VWF bind to collagen through their I-domains, in VWF known as A-domains (13–19). A-domains form independent globular modules of some 200 amino acid residues. In VWF three such domains have been identified. The A1-domain contains the binding site for glycoprotein Ib (20, 21), sulfatides (22), heparin (23), and collagen VI (24, 25), which constitutes the main reactive collagen in the extracellular matrix of endothelial cells. The A2-domain has no clear binding function but is sensitive to protease ADAMTS13-mediated enzymatic degradation (26, 27), whereas the A3-domain (residues 920–1111) contains the main binding site for fibrillar collagens such as type I and III (19, 28). Recombinant A3-domain also binds to collagen (28), whereas deletion of A3 results in a VWF that binds 40 times less to collagen (19). By using synthetic triple helical collagen-related peptides, the VWF-binding site has been localized to residues 541–558 of the $\alpha1CB4(III)$ fragment of collagen type III (29). Recently, we identified the collagen binding site by cocrystallization of the A3-domain with an inhibitory anti-A3 antibody, RU5, which was confirmed by showing that especially an H1023A mutant abolished binding of VWF to collagen (30). This study was further extended by the analysis of a series of 27 VWF-A3 mutants, which defined the collagen binding site of the VWF-A3-domain to the "front" face of the domain (31), an observation confirmed by Nishida *et al.* (32).

We raised a monoclonal antibody (mAb), 82D6A3, against human VWF that prevents the binding of VWF to collagen (24) and that is antithrombotic in a baboon arterial thrombosis model (33). Since a previous effort to determine the epitope of 82D6A3 using phage display, was not successful (34, 35), we repeated this study using less stringent selection criteria. Us-

[1] The abbreviations used are: VWF, von Willebrand factor; mAb, monoclonal antibody; HRP, horseradish peroxidase; GAM-HRP, goat anti-mouse IgG labeled with horseradish peroxidase; PBS, phosphate-buffered saline.

ing phage display together with mutagenesis studies, we now identified the epitope of mAb 82D6A3. Moreover, we demonstrate that the structure of the consensus sequence in a selected cyclic 6-mer peptide mimics the discontinuous epitope in the VWF A3-domain. To the best of our knowledge, this is the first report where modeling of a consensus sequence in a cyclic 6-mer peptide indicates that it indeed adopts the conformation of the antigen and thereby can represent the discontinuous epitope.

EXPERIMENTAL PROCEDURES

Materials—Human placental collagen type I and III were purchased from Sigma. The collagens were solubilized in 50 mmol/liter acetic acid and subsequently dialyzed against phosphate-buffered saline PBS (48 h, 4 °C) to obtain fibrillar collagen. A phage display library with random hexapeptides flanked by cysteine residues was obtained from Corvas (Gent, Belgium), and a pentadecamer phage display peptide library was a kind gift of Dr. G. Smith (University of Missouri, Columbia, MO). VWF was purchased from the Red Cross Belgium. mAb and phages were biotinylated using *N*-hydroxysuccinimide-LC-Biotin (Pierce) according to the manufacturer's instructions.

Preparation of 82D6A3 and Its Fab Fragments—82D6A3, raised against human VWF, was purified from murine ascites by Protein A chromatography. 82D6A3-Fab was prepared by digestion with papain. Briefly, 5 mg of mAb was digested with 50 μg of papain (Sigma) in the presence of 10 mmol/liter cysteine and 50 mmol/liter EDTA (37 °C, overnight). The Fab fragments were purified by protein A affinity chromatography (Amersham Biosciences), and purity was checked by SDS-PAGE.

Binding of 82D6A3 to Different Forms of VWF—A 96-well plate (Greiner, Frickenhausen, Germany) was coated overnight with VWF (Red Cross), A3-domain of VWF, or ΔA3-VWF (10 μg/ml in PBS) and blocked with 3% milk powder solution. A dilution series of 82D6A3 (in 0.3% milk powder solution) was added for 1.5 h, bound mAb was detected for 1 h with goat anti-mouse IgG labeled with horseradish peroxidase (GAM-HRP) (Sigma) (1:10,000 in PBS, 0.3% milk powder), and visualization was performed using H_2O_2 and *ortho*-phenylenediamine (Sigma). The reaction was stopped with 4 mol/liter H_2SO_4, and absorbance was determined at 490 nm. In between each incubation step, the plates were washed 3–9 times with PBS, 0.1% Tween 20 (PBST).

Inhibition of VWF Binding to Collagen by 82D6A3 and Its Fab Fragments—A 96-well plate (Greiner, Frickenhausen, Germany) was coated overnight with human collagen type I (25 μg/ml in PBS) and blocked with 3% milk powder solution. Purified human VWF (0.5 μg/ml final concentration) was preincubated with a dilution series of 82D6A3 or its Fab fragments during 30 min before the addition to the collagen-coated plate. After a 90-min incubation, bound VWF was detected with a polyclonal anti-VWF-Ig solution conjugated with horseradish peroxidase (Dako, Glostrup, Denmark) (1:3000 in PBS, 0.3% milk powder), and visualization was performed as described above. In between each incubation step, the plates were washed 3–9 times with PBST.

Flow Experiments—Flow experiments were performed in a parallel plate flow chamber with a slit height of 0.4 mm as described (36). Briefly, blood was taken from healthy volunteers, who had not taken aspirin or analogues for the last 10 days, on 0.313% citrate. Thermanox coverslips (Nunc, Rochester, NY) were coated with human fibrillar collagen type III (1 mg/ml, 100 μl/coverslip). The perfusion chamber and tubings were blocked with a 1% bovine serum albumin, 0.1% glucose solution for 20 min and washed with Hepes-buffered saline before starting the experiment. In each experiment, 15 ml of blood, preincubated for 15 min with 82D6A3, was perfused for 5 min. After the perfusion, coverslips were rinsed with Hepes-buffered saline and incubated in 0.5% glutardialdehyde (10 min). Next, the coverslips were placed in methanol (5 min), stained with May-Grünwald (3–5 min) and Giemsa (15–20 min), and washed two times with distilled water. Coverslips were dried and analyzed with an image analyzer as described (36). The perfusion experiments were performed at wall shear rates of 650 s^{-1}, 1300 s^{-1}, and 2600 s^{-1}.

Isolation of mAb Binding Phages—To further identify the epitope of 82D6A3, a linear pentadecamer and a cyclic hexamer phage display library were used. Biotinylated mAb (10 μg) was bound to blocked streptavidin-coated magnetic beads (Dynal, Oslo, Norway). First, $2 \cdot 10^{12}$ phages (PBS, 0.2% milk powder) were incubated with blocked streptavidin-coated beads for 1 h to eliminate streptavidin-binders. Next,

phages were added to the 82D6A3-containing beads. After 90 min, beads were washed 10 times with PBST. When using the linear pentadecamer library, in the first panning round, bound phages were eluted with 0.1 mol/liter glycine, pH 2.2, and the eluate was immediately neutralized with 1 mol/liter Tris-HCl, pH 8. After amplification of the phages, two additional rounds of panning were performed where bound phages were eluted using the recombinant A3-domain of VWF (20 μg/ml). Using the cyclic hexamer library, four panning rounds were performed, and each time a nonspecific elution with glycine was performed. After all panning rounds, phages were amplified by infection of *Escherichia coli* TG1 cells and partially purified from the supernatant by polyethylene glycol precipitation. Enrichment of 82D6A3 binding phages over the panning rounds was tested in an enzyme-linked immunosorbent assay (see below). After the last panning round, a dilution of the eluted phage pool was plated on Luria Broth (LB) agar plates containing tetracycline. Single colonies were picked from these plates and were grown overnight in 2× TY medium containing tetracycline in a 96-well plate, plates were centrifuged, and the phage-containing supernatant was tested for the presence of 82D6A3-binding phages in enzyme-linked immunosorbent assay (see below). Phage DNA was prepared by phenol/chloroform extraction, and sequencing reactions were performed using the Sequenase version 2.0 DNA Sequencing Kit (Amersham Biosciences) using [^{35}S]dATP according to the manufacturer's instructions. For the linear pentadecamer phages, primer 5′-CTCATA-GTTAGCGTAACG-3′ was used, and for the cyclic hexamer phages, 5′-CCCTCATAGTTAGCGTAACG-3′ was used.

Measurement of Phage Binding to 82D6A3—A 96-well plate was coated overnight with purified 82D6A3 (10 μg/ml in PBS). After 2 h of blocking with a 2% milk powder solution, a dilution series of either a phage solution obtained after the different rounds of panning or the individual phage clones selected after the final panning round were added to the wells (all in PBS with 0.2% milk powder), and phages were incubated at room temperature for 90 min. Bound phages were detected after a 1-h incubation with a polyclonal anti-M13-HRP-conjugated antibody (Amersham Biosciences), and visualization was performed as described above. After all incubation steps, plates were washed with PBS, 0.1% Tween 20.

Specificity of Phage Binding to 82D6A3—A 96-well plate was coated overnight with purified 82D6A3 (10 μg/ml in PBS). After blocking with 2% milk powder for 2 h, a dilution series of VWF or recombinant A3-domain in PBS, 0.2% milk powder was added. After a 30-min preincubation, a constant amount of phages (PBS, 0.2% milk powder) was added to the VWF/A3-containing wells. After 90 min, bound phages were detected as described above.

Competition between different phage clones for binding to 82D6A3 was analyzed as above, except that $2 \cdot 10^{10}$/ml biotinylated phages of clone 1 were mixed with various concentrations of phages from clone 2, after which bound biotinylated phages were detected with streptavidin-HRP and *ortho*-phenylenediamine.

Immunoblotting of Phages—Purified phages ($2 \cdot 10^{10}$) were analyzed on a 10% SDS-PAGE gel under nonreducing and reducing conditions and blotted to a nitrocellulose membrane (Schleicher and Schuell). After blocking the membrane with a 4% milk powder solution, the membrane was incubated with 82D6A3 (2 μg/ml in PBS, 0.4% milk powder) during 90 min, followed by a 1-h incubation with GAM-HRP (Sigma). The membrane was developed using the ECL detection system (Amersham Biosciences). After each incubation step, the membrane was washed with PBS containing 0.05% Tween 80.

Expression, Purification, and Characterization of VWF—The construction and purification of VWF mutants with point mutations in the A3-domain has been described (30, 31). Briefly, VWF was stably expressed in fur-BHK cells and purified by immunoaffinity chromatography using monoclonal antibody RU8. VWF concentration was determined by a sandwich enzyme-linked immunosorbent assay, and its multimeric structure was analyzed by agarose gel electrophoresis followed by Western blotting.

Binding of 82D6A3 to VWF Mutants—Microtiter plate wells (Costar, Cambridge, MA) were coated with a 2.5 μg/ml concentration of a polyclonal antibody directed against the D′- and D3-domains of VWF (37) in 50 mM carbonate buffer, pH 9.6, and blocked with 3% bovine serum albumin in PBS, 0.1% Tween 20. Wells were incubated with expression medium diluted with PBS, 0.1% Tween 20, 3% bovine serum albumin to a final VWF concentration of 100 ng/ml for 60 min at 37 °C. Next, 5 μg/ml 82D6A3 was added, and bound antibodies were detected with HRP-conjugated rabbit anti-mouse antibodies (DAKO, 1:2500 in PBS, 0.1% Tween 20, 3% bovine serum albumin). *ortho*-Phenylenediamine was used as substrate for detection as described above. Between each incubation step, wells were washed with PBST.
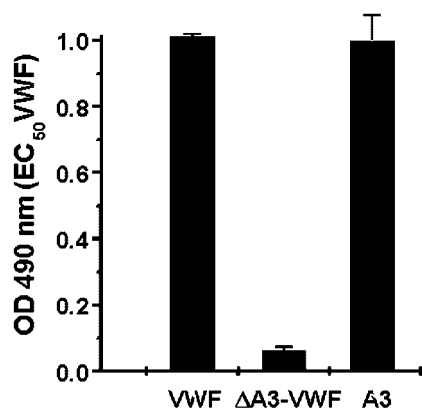
FIG. 1. **Binding of mAb 82D6A3 to different forms of VWF.** Dilution series of mAb 82D6A3 were added to VWF, A3-domain, or ΔA3-VWF-coated wells, and bound 82D6A3 was detected with GAM-HRP. The A_{490} corresponding with the EC_{50} value of 82D6A3 binding to VWF was used as a reference to determine the A_{490} for 82D6A3 binding to the A3-domain and to ΔA3-VWF. Data are the mean ± S.D. ($n = 3$).

Modeling and Mapping of a 82D6A3-binding Peptide—The structure of the cyclic peptide CMTSPWRC was modeled using the Brugel modeling package (38). First, the linear sequence was generated and during a constrained minimization step, the peptide was cyclicized via SS bonding. Next, 20,000 steps of unconstrained molecular dynamics simulation were performed to explore the conformational space of the free cyclic peptide. The lowest energy structure was selected and manually fitted onto the VWF A3-domain. The main and side chain atoms of the Ser and Arg residues were used as anchors to superimpose the structures.

RESULTS

Characterization of 82D6A3 and Its Fab Fragments under Static and Flow Conditions—mAb 82D6A3, an anti-human VWF antibody, and its Fab fragments inhibit binding of purified VWF to human collagen type I in a specific and dose-dependent manner with an IC_{50} of 20 ng/ml for the IgG and 1 μg/ml for the Fab fragments. mAb 82D6A3 recognizes the A3-domain of VWF as it binds to the recombinant VWF A3-domain but not to ΔA3-VWF (Fig. 1) (24, 35). Moreover, the conformation of VWF is important for 82D6A3 binding as the mAb recognizes denatured VWF but not reduced and denatured VWF (not shown).

82D6A3 also inhibited platelet adhesion under flow conditions at different shear rates. At a shear rate of 2600 s^{-1}, 82D6A3 completely inhibited platelet deposition at concentrations of 2.3 μg/ml (Fig. 2A). The inhibitory effect increased with increasing shear stress, in agreement with the VWF dependence of the reaction (Fig. 2B).

Epitope Mapping of 82D6A3 Using Phage Display—Two peptide phage display libraries, a linear pentadecamer and a cyclic hexamer, were used. After three rounds of biopanning, 96 individual clones were grown and tested for their ability to bind to 82D6A3. Seven phage clones were positive, of which clones G8, G2, and C2 had a similar affinity for 82D6A3, clone C5 had a slightly lower affinity (Fig. 3A), and three clones had a low affinity and were not further investigated. Furthermore, both types of phage clones inhibited VWF binding (Fig. 3B) and A3-domain binding (not shown) to 82D6A3 to the same extent, demonstrating that the phages were binding to the antigen binding site of the antibody and could thus represent an epitope or mimotope of 82D6A3. From these four clones, the sequence was determined, which resulted in the identification of two sequences: GDCFFGFLN**SPWR**VC (L15G8, G2, C2) and RSSYWVY**SPWR**FISR (L15C5). Both sequences share the 4-amino acid sequence SPWR.

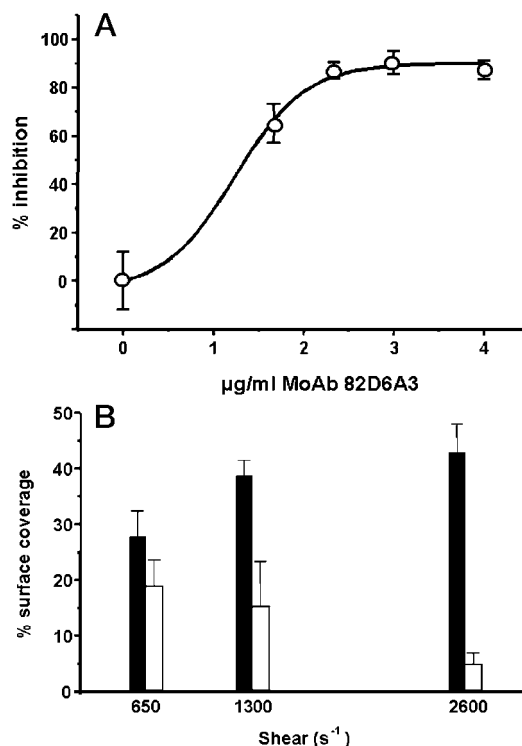After four rounds of biopanning with the cyclic hexamer

FIG. 2. **Effect of 82D6A3 on platelet adhesion under flow conditions.** Platelet deposition onto a human collagen type III-coated surface was studied as a function of the concentration of mAb 82D6A3 at a shear rate 2600 s^{-1} (*A*) and as a function of the shear rate (*B*). *Closed bars*, no antibody; *open bars*, 2.3 μg/ml 82D6A3. Data are mean ± S.D. ($n = 4$, with blood from two different donors).

library and nonspecific elution, 94 individual clones were checked for binding to 82D6A3, of which 13 were positive. All of these phage clones inhibited the VWF binding to 82D6A3. Eight of the 13 clones displayed the sequence CMT**SPWR**C (C6H5), four displayed the sequence CRT**SPWR**C (C6G12), and one had a CYR**SPWR**C (C6A12) sequence. These sequences thus also contained the SPWR sequence, and indeed the L15G8 and C6H5 phage did compete with each other for binding to 82D6A3 (Fig. 4). Furthermore, 82D6A3 was only able to recognize the L15G8 and C6H5 phages when blotted under nonreducing conditions and not when the disulfide bond was reduced, pointing out that the two cysteines present in both clones are forming a disulfide bridge and that the structure of the conformational constrained peptide is thus necessary for recognition by 82D6A3 (Fig. 4, *inset*).

All of the selected peptide sequences were aligned to the VWF-A3 sequence using ClustalW using all of the program default values (39) (available on the World Wide Web at www.ebi.ac.uk/clustalw/). With this program, progressive multiple sequence alignments are performed, and the alignment is built up in stages where a new sequence is added to an existing alignment through sequence weighting, position-specific gap penalties, and weight matrix choice (39). Multiple sequence alignment of all of the peptide sequences with the VWF A3-domain sequence or sequence alignment of each peptide sequence separately with the VWF A3-domain sequence always resulted in positioning of the peptide sequences at the PW sequence (positions 981 and 982) in the VWF A3-domain (Table I). This particular PW sequence is only present once in the VWF A3-domain. However, more similarity was not identified, as expected, since 826A3 does not have a linear epitope. Thus, the SPWR consensus sequence might mimic the epitope, presumably bearing similarity to its three-dimensional structure.

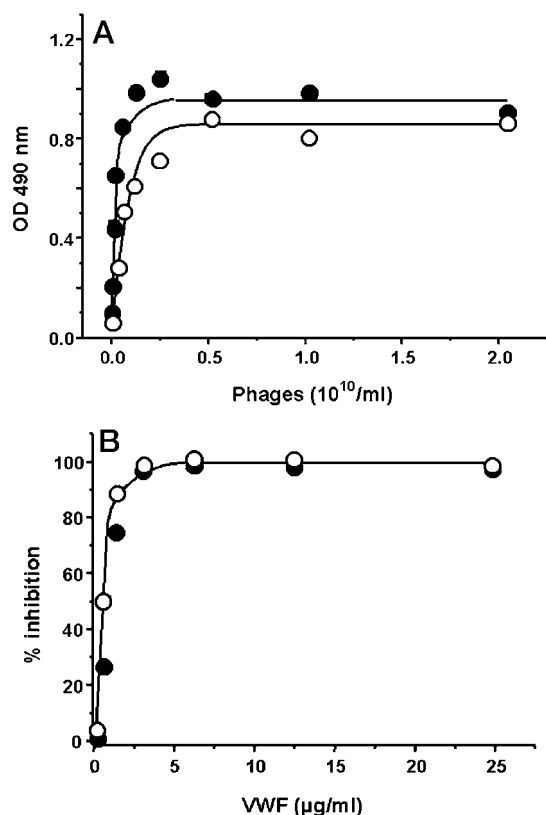*Epitope Mapping of 82D6A3 by Mutant VWF Analysis*—To

FIG. 3. **Selection of phages interacting with the antigen binding pocket of 82D6A3.** *A*, dose-dependent binding of phage clone L15G8 (●) and L15C5 (○) to 82D6A3. Bound phages were detected with polyclonal anti-M13-HRP antibodies. *B*, inhibition of the binding of phage clones L15G8 (●) and L15C5 (○) to 82D6A3 by VWF. Phages (final concentration: 8·10⁹ phages/ml) and a dilution series of VWF were preincubated for 30 min before the addition to the 82D6A3-coated plate. Bound phages were detected with polyclonal anti-M13-HRP antibodies.
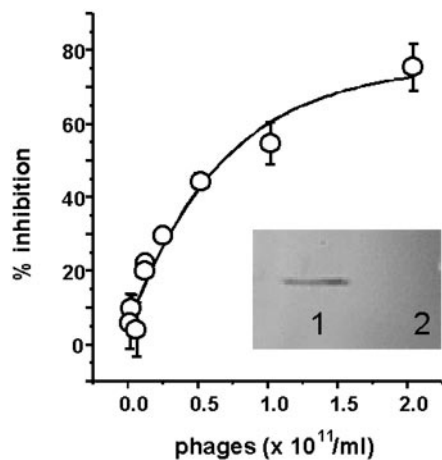

FIG. 4. **Characterization of the L15 and C6 phages.** Binding of biotinylated C6H5-phages to 82D6A3 was inhibited by L15G8 phages. C6H5 phages were used at a final concentration of 2·10¹⁰/ml. Bound biotinylated C6H5 phages were detected with streptavidin-HRP. *Inset*, phages (2·10¹⁰) were analyzed in SDS-PAGE using a 10% gel under nonreducing (*lane 1*) and reducing (*lane 2*) conditions. Proteins were transferred to a nitrocellulose membrane, and detection was performed using 82D6A3 followed by the addition of GAM-HRP.

further unravel the epitope of 82D6A3, binding of 82D6A3 to different VWF mutants was analyzed. The VWF mutants containing mutations in the A3-domain were previously constructed to identify the collagen-binding region within the A3-domain (30, 31). Both 82D6A3 (Fig. 5) and RU5 bind to

TABLE I
Alignment of selected peptide sequences with part of the VWF A3 domain sequence

The SPWR consensus sequence in the selected peptides is in boldface type, the PW sequence is identified by alignment between the peptide sequences and the VWF A3 domain sequence, and is boldface and underlined.

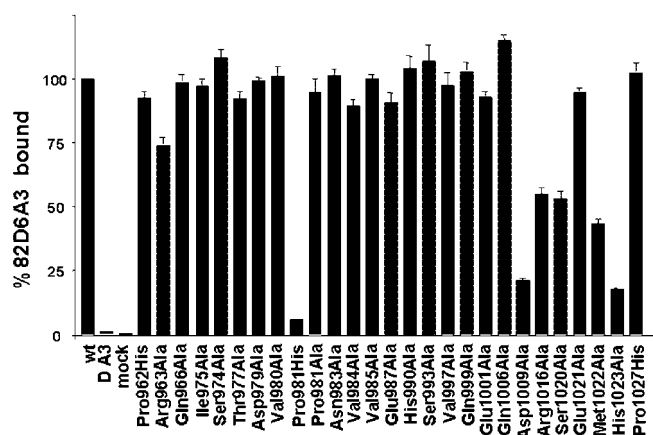| Peptide	Sequence
L15G8	GDCFFGFLN**SPWR**VC
L15C5	RSSYWVY**SPWR**FISR
C6H5	CMT**SPWR**C
C6G12	CRT**SPWR**C
C6A12	CYR**SPWR**C
VWF A3 domain	^{967}VSVLQYGSITTIDV**PW**NVVPEKAH^{990}

FIG. 5. **Binding of 82D6A3 to wild type VWF, ΔA3-VWF, and VWF with the indicated mutations in the A3-domain.** VWF and its mutants are captured with polyclonal anti-VWF antibodies, 5 µg/ml 82D6A3 was added, and bound mAb was detected with rabbit anti-mouse antibodies conjugated with HRP. Values are expressed as percentage of binding to wild type VWF (mean ± S.D., n = 3).

recombinant wild type VWF and not to ΔA3-VWF and compete with each other for binding (30).

Next, binding of 82D6A3 to these 27 VWF mutants was studied, and a number of residues important for antibody recognition were identified (Fig. 5). The mutant P981H no longer bound to 82D6A3; however, mutant P981A bound normally. 82D6A3 bound less (residual binding of less than 75% binding) to VWF with Ala mutations of residues Arg^{963}, Asp^{1009}, Arg^{1016}, Ser^{1020}, Met^{1022}, and His^{1023} (Fig. 5).

Interestingly, the effects of the various mutants on 82D6A3 binding correlates well with the effect on collagen binding. We previously demonstrated that of these 27 VWF mutants used, R963A, I975A, T977A, D979A, P981H, V997A, E1001A, R1016A, S1020A, and H1023A all reduced collagen binding (30, 31). Comparison of the effects of the various mutants on 82D6A3 binding and on collagen binding revealed that of these mutants, R963A, P981H, R1016A, S1020A, and H1023A also had a reduced binding to 82D6A3 (Fig. 6).

Modeling of a Peptide Containing the SPWR Consensus Sequence—Identification of the residues important in 82D6A3 recognition by mutant analysis suggested that the SPWR consensus sequence identified by phage display might represent amino acids Ser^{1020}, Pro^{981}, Trp^{982}, and Arg^{1016} in the VWF A3-domain. Inspection of these residues in the three-dimensional structure of the A3-domain demonstrated that these residues are indeed close together in space (Fig. 7).

The structure of the cyclic peptide CMTSPWRC was modeled and mapped onto the VWF-A3 structure (Fig. 8). An acceptable superposition was obtained where the Ser and Arg from the

peptide superimpose with A3 residues Ser[1020] and Arg[1016], with the Pro residue serving as a spacer that correctly orients the Ser and Arg residues. The side chains of the Trp in the cyclic peptide and Trp[982] in VWF could be mapped, provided the latter is rotated in such a way that it becomes exposed to the solvent (Fig. 8). This indicates that the linear SPWR sequence actually mimics the conformation of the epitope.

DISCUSSION

The anti-VWF mAb 82D6A3 and its Fab fragments are potent inhibitors of the VWF-collagen interaction under both static and flow conditions. We recently demonstrated that inhibiting the VWF-collagen interaction by 82D6A3 results in an effective antithrombotic therapy when tested in baboons using a modified Folts model in the femoral artery (33), thereby confirming that the VWF-collagen interaction has a relevant physiological role.

82D6A3 binds to the A3-domain of VWF but not to denatured and reduced VWF, pointing out that the mAb does not recognize a linear epitope. To determine the epitope of 82D6A3 more accurately, we used phage display technology, mutagenesis,
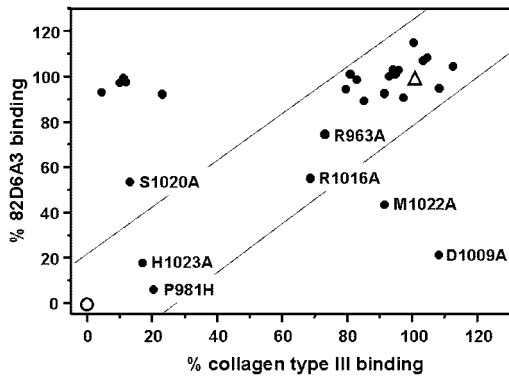
and computer modeling. Selection of antibody-binding phages from a pentadecamer and cyclic hexamer phage display library resulted in phages that bind to 82D6A3 in a dose-dependent manner. Moreover, VWF and the recombinant A3-domain were able to inhibit phage binding to the mAb, indicating that the phages bind at or near the antigen-binding site of 82D6A3. Sequence comparison of the phage-displayed peptides revealed a consensus SPWR sequence in all phages selected. Using the ClustalW program, the SPWR-sequence was aligned to the PW
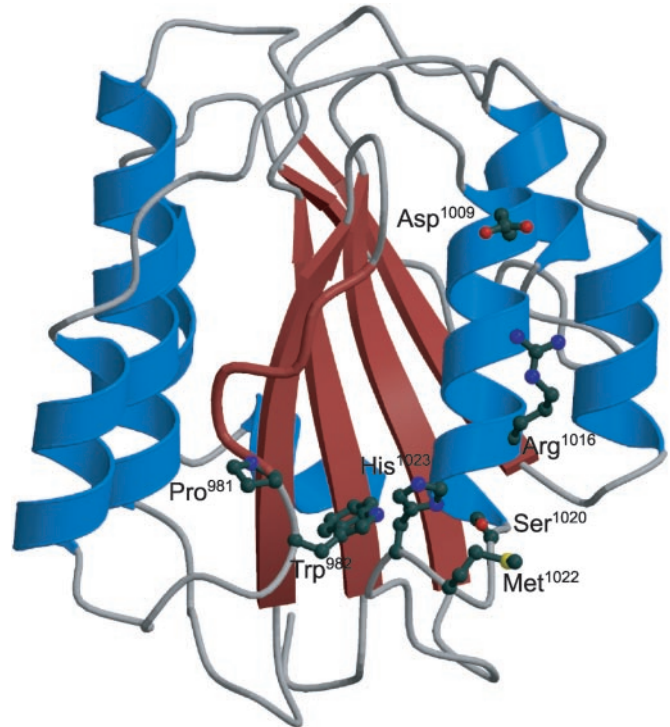

FIG. 6. **Correlation between the effects of VWF mutations on 82D6A3 binding and collagen binding.** Percentage of binding to 82D6A3 and to collagen type III of ΔA3-VWF (○) and VWF A3-domain mutants (●) is represented. Binding to wild type VWF (△) was set as 100%.

FIG. 7. **Location of dominant 82D6A3 epitope amino acid residues within the VWF-A3-domain.** Coordinates of the crystal structure of the VWF A3 domain were taken from Protein Data Bank entry 1ATZ.
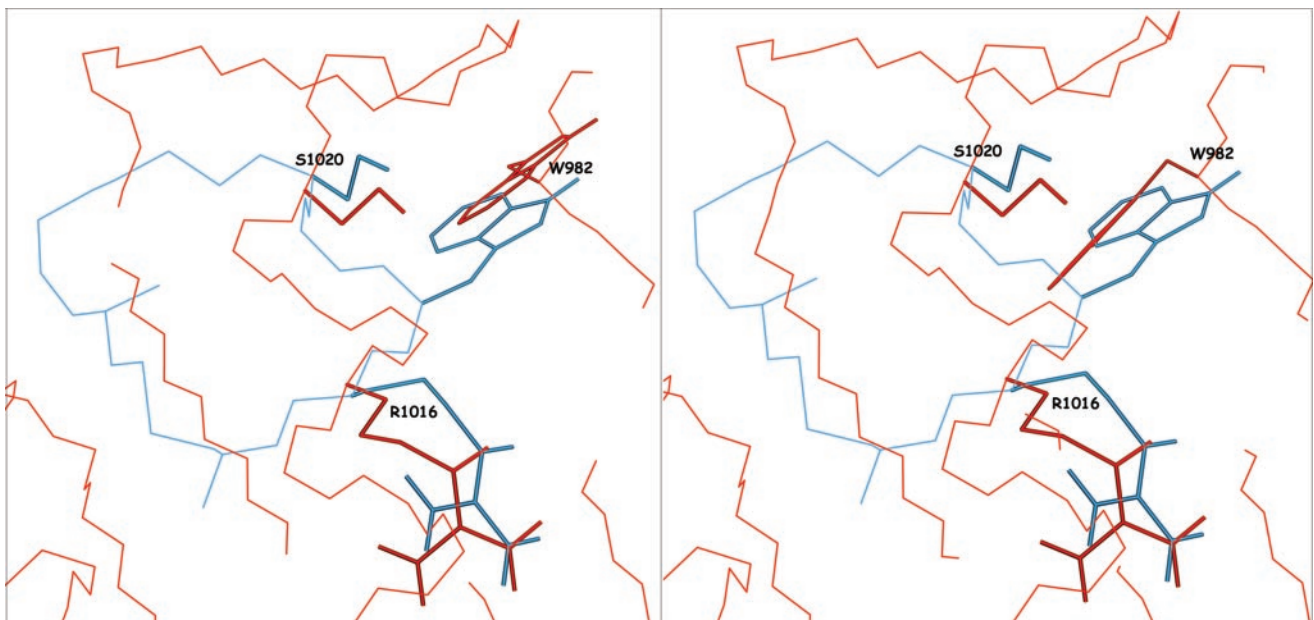

FIG. 8. **Superposition of the modeled cyclic CMTSPWRC onto the structure of VWF-A3.** *Right panel*, the cyclic CMTSPWRC peptide (*blue*, with Arg, Ser, and Trp in *dark blue*) was modeled using the Brugel modeling package and was subsequently fitted onto the VWF-A3-structure (*red*). Amino acid residues Arg[1016] and Ser[1020] within the VWF A3-domain are in *bold red*. The *left panel* shows the "exposed form" of Trp[982] in close vicinity and orientation of the cyclic Trp in the cyclic hexapeptide.

sequence (amino acids 981 and 982) within the A3-domain.

To confirm and to further unravel the epitope, the binding of 82D6A3 to a series of VWF mutants was studied. When Pro[981] was mutated to His, binding of VWF to 82D6A3 was indeed lost, as was the binding to collagen. However, mutant P981A interacted normally with both 82D6A3 and collagen, implying that Pro[981] is not directly involved in binding. Apparently, the introduction of a much larger histidine side chain at this position blocks the binding of 82D6A3 and A3 by steric hindrance. However, Nishida *et al.* (32) reported an important decrease in collagen binding of the P982A mutant, but they used isolated A3-domain mutants, whereas we expressed the full-length VWF protein. Apart from the P981H mutation, mutation of Arg[963], Asp[1009], Arg[1016], Ser[1020], Met[1022], and His[1023] to alanine also affected 82D6A3 binding with R963A, R1016A, S1020A, and H1023A previously reported to result in a reduced collagen binding (30, 31). We next modeled the cyclic 6-mer peptide CMTSPWRC and superimposed its SPWR consensus sequence on the VWF A3-domain structure, demonstrating that the consensus tetrapeptide can indeed mimic the three-dimensional structure of the epitope.

The successful use of phage display for the identification of linear epitopes has been well described (40–43). In most cases, phages are selected that display consensus sequences that can be aligned with the primary sequence of the antigen, thus identifying the original epitope. The use of phage display to map discontinuous or conformational epitopes, however, is not so obvious, since it is difficult to mimic such epitopes with a linear sequence. To increase the probability of identifying such epitopes, constrained libraries, where a disulfide bond between two half-cystine residues at fixed positions is present, or libraries with long peptides (>20 amino acids) were developed (41–43). Only a few reports are available where the consensus sequence of the identified displayed peptides could be tentatively positioned in the crystal structure or the modeled structure of the antigen and thus point out that these residues might represent the epitope of the antibody (44–49). However, we are not aware of any reports where a modeled peptide containing the consensus sequence could actually be fitted on the structure of the antigen. We here not only could show that the distance between the C-α atoms of the Ser and Arg in the peptide compares well with those of the Ser[1020] and Arg[1016] (0.42 and 0.34 Å, respectively) but that also the relative orientation is comparable. The Pro residue of the peptide does not match with Pro[981] and hence serves as a spacer to correctly orient the Ser and Arg of the peptide. For the Trp, the side chain points in the direction of Trp[982] (Fig. 8, *right panel*). According to simulations, the side chain of Trp[982] could rotate in such a way that it becomes exposed to the solvent and overlaps then with the Trp in the peptide (Fig. 8, *left panel*). However, this requires further experimental confirmation. In conclusion, identification of the consensus sequence SPWR, modeling of a cyclic 6-mer peptide containing this sequence, and superposition on the VWF A3-domain revealed that the SPWR sequence may adopt a conformation that corresponds with a dominant discontinuous epitope of 82D6A3, where the Ser and Arg mimic Ser[1020] and Arg[1016]. The Pro serves as a spacer, and the Trp is either a spacer residue or might mimic Trp[982] if the latter residue is solvent-exposed.

Finally, the studies with VWF mutants also revealed that the effects of mutations R963A, R1016A, S1020A, H1023A, and P981H on 82D6A3 binding correlate with the effect on collagen binding (in addition to Ile[975], Thr[977], Asp[979], Val[997], and Glu[1001]). This demonstrates that 82D6A3 interacts with amino acids in the VWF A3-domain critical for collagen binding and that 82D6A3 does not inhibit the VWF collagen interaction through steric hindrance.

REFERENCES

1. Santoro, S. A. (1986) *Cell* **46,** 913–920
2. Nieuwenhuis, H. K., Akkerman, J. W., Houdijk, W. P., and Sixma, J. J. (1985) *Nature* **318,** 470–472
3. Beer, J. H., Rabaglio, M., Berchtold, P., von Felten, A., Clemetson, K. J., Tsakiris, D. A., Kehrel, B., and Brandenberger, S. (1993) *Blood* **82,** 820–829
4. Arai, M., Yamamoto, N., Moroi, M., Akamatsu, N., Fukutake, K., and Tanoue, K. (1995) *Br. J. Haematol.* **89,** 124–130
5. Clemetson, J. M., Polgar, J., Magnenat, E., Wells, T. N., and Clemetson, K. J. (1999) *J. Biol. Chem.* **274,** 29019–29024
6. Berndt, M. C., Shen, Y., Dopheide, S. M., Gardiner, E. E., and Andrews, R. K. (2001) *Thromb. Haemost.* **86,** 178–188
7. Sixma, J. J., and de Groot, P. G. (1991) *Mayo Clin. Proc.* **66,** 628–633
8. Goto, S., Salomon, D. R., Ikeda, Y., and Ruggeri, Z. M. (1995) *J. Biol. Chem.* **270,** 23352–23361
9. Savage, B., Almus-Jacobs, F., and Ruggeri, Z. M. (1998) *Cell* **94,** 657–666
10. Moroi, M., Jung, S. M., Nomura, S., Sekiguchi, S., Ordinas, A., and Diaz-Ricart, M. (1997) *Blood* **90,** 4413–4424
11. Kehrel, B., Wierwille, S., Clemetson, K. J., Anders, O., Steiner, M., Knight, C. G., Farndale, R. W., Okuma, M., and Barnes, M. J. (1998) *Blood* **91,** 491–499
12. Schoolmeester, A., Vanhoorelbeke, K., Lecut, C., Heemskerk J., Hoylaerts, M., and Deckmyn H. (2003) *J. Thromb. Haemost.* **1,** Suppl. 1, OC139 (abstr.)
13. Santoro, S. A., and Zutter, M. M. (1995) *Thromb. Haemost.* **74,** 813–821
14. Kamata, T., Puzon, W., and Takada, Y. (1994) *J. Biol. Chem.* **269,** 9659–9663
15. Kamata, T., and Takada, Y. (1994) *J. Biol. Chem.* **269,** 26006–26010
16. Bahou, W. F., Potter, C. L., and Mirza, H. (1994) *Blood* **84,** 3734–3741
17. Depraetere, H., Wille, C., Gansemans, Y., Stanssens, P., Lauwereys, M., Baruch, D., De Reys, S., and Deckmyn, H. (1997) *Thromb. Haemostasis* **77,** 981–985
18. Colombatti, A., and Bonaldo, P. (1991) *Blood* **77,** 2305–2315
19. Lankhof, H., van Hoeij, M., Schiphorst, M. E., Bracke, M., Wu, Y. P., Ijsseldijk, M. J., Vink, T., de Groot, P. G., and Sixma, J. J. (1996) *Thromb. Haemostasis* **75,** 950–958
20. Mohri, H., Zimmerman, T. S., and Ruggeri, Z. M. (1993) *Peptides* **14,** 125–129
21. Sixma, J. J., Schiphorst, M. E., Verweij, C. L., and Pannekoek, H. (1991) *Eur. J. Biochem.* **196,** 369–375
22. Christophe, O., Obert, B., Meyer, D., and Girma, J. P. (1991) *Blood* **78,** 2310–2317
23. Sobel, M., Soler, D. F., Kermode, J. C., and Harris, R. B. (1992) *J. Biol. Chem.* **267,** 8857–8862
24. Hoylaerts, M. F., Yamamoto, H., Nuyts, K., Vreys, I., Deckmyn, H., and Vermylen, J. (1997) *Biochem. J.* **324,** 185–191
25. Mazzucato, M., Spessotto, P., Masotti, A., De Appollonia, L., Cozzi, M. R., Yoshioka, A., Perris, R., Colombatti, A., and De Marco, L. (1999) *J. Biol. Chem.* **274,** 3033–3041
26. Lankhof, H., Damas, C., Schiphorst, M. E., Ijsseldijk, M. J., Bracke, M., Furlan, M., Tsai, H. M., de Groot, P. G., Sixma, J. J., and Vink, T. (1997) *Thromb. Haemostasis* **77,** 1008–1013
27. Zheng, X., Chung, D., Takayama, T. K., Majerus, E. M., Sadler, J. E., and Fujikawa, K. (2001) *J. Biol. Chem.* **276,** 41059–41063
28. Cruz, M. A., Yuan, H., Lee, J. R., Wise, R. J., and Handin, R. I. (1995) *J. Biol. Chem.* **270,** 19668
29. Verkleij, M. W., Ijsseldijk, M. J., Heijnen-Snyder, G. J., Huizinga, E. G., Morton, L. F., Knight, C. G., Sixma, J. J., de Groot, P. G., and Barnes, M. J. (1999) *Thromb. Haemostasis* **82,** 1137–1144
30. Romijn, R. A., Bouma, B., Wuyster, W., Gros, P., Kroon, J., Sixma, J. J., and Huizinga, E. G. (2001) *J. Biol. Chem.* **276,** 9985–9991
31. Romijn, R. A., Westein, E., Bouma, B., Schiphorst, M. E., Sixma, J. J., Lenting, P. J., and Huizinga, E. G. (2003) *J. Biol. Chem.* **278,** 15035–15039
32. Nishida, N., Sumikawa, H., Sakakura, M., Shimba, N., Takahashi, H., Terasawa, H., Suzuki, E. I., and Shimada, I. (2003) *Nat. Struct. Biol.* **10,** 53–58
33. Wu, D., Vanhoorelbeke, K., Cauwenberghs, N., Meiring, M., Depraetere, H., Kotze, H. F., and Deckmyn, H. (2002) *Blood* **99,** 3623–3628
34. Depraetere, H., Viaene, A., Deroo, S., Vauterin, S., and Deckmyn, H. (1998) *Blood* **92,** 4207–4211
35. Vanhoorelbeke, K., van der Plas, R. M., Vandecasteele, G., Vauterin, S., Huizinga, E. G., Sixma, J. J., and Deckmyn, H. (2000) *Thromb. Haemostasis* **84,** 621–625
36. Harsfalvi, J., Stassen, J. M., Hoylaerts, M. F., Van Houtte, E., Sawyer, R. T., Vermylen, J., and Deckmyn, H. (1995) *Blood* **85,** 705–711
37. van der Plas, R. M., Gomes, L., Marquart, J. A., Vink, T., Meijers, J. C., de Groot, P. G., Sixma, J. J., and Huizinga, E. G. (2000) *Thromb. Haemostasis* **84,** 1005–1011
38. Delhaise, P., Bardiaux, M., De Maeyer, M., Prevost, M., Vanbelle, D., Donneux, J., Lasters, I., Vancustem, E., Alard, P., and Wodak, S. J. (1988) *J. Mol. Graphics* **6,** 219
39. Thompson, J. D., Higgins, D. G., and Gibson, T. J. (1994) *Nucleic Acids Res.* **22,** 4673–4680
40. Scott, J. K., and Smith, G. P. (1990) *Science* **249,** 386–390
41. Yip, Y. L., and Ward, R. L. (1999) *Comb. Chem. High Throughput Screen.* **2,** 125–138

42. Smith, G. P., and Petrenko, V. A. (1997) *Chem. Rev.* **97,** 391–410
43. Cortese, R., Felici, F., Galfre, G., Luzzago, A., Monaci, P., and Nicosia, A. (1994) *Trends Biotechnol.* **12,** 262–267
44. Villard, S., Piquer, D., Raut, S., Leonetti, J. P., Saint-Remy, J. M., and Granier, C. (2002) *J. Biol. Chem.* **277,** 27232–27239
45. Demangel, C., Maroun, R. C., Rouyre, S., Bon, C., Mazie, J. C., and Choumet, V. (2000) *Eur. J. Biochem.* **267,** 2345–2353
46. Myers, M. A., Davies, J. M., Tong, J. C., Whisstock, J., Scealy, M., Mackay, I. R., and Rowley, M. J. (2000) *J. Immunol.* **165,** 3830–3838
47. Luzzago, A., Felici, F., Tramontano, A., Pessi, A., and Cortese, R. (1993) *Gene (Amst.)* **128,** 51–57
48. Furmonaviciene, R., Tighe, P. J., Clark, M. R., Sewell, H. F., and Shakib, F. (1999) *Clin. Exp. Allergy* **29,** 1563–1571
49. Ravera, M. W., Carcamo, J., Brissette, R., Alam-Moghe, A., Dedova, O., Cheng, W., Hsiao, K. C., Klebanov, D., Shen, H., Tang, P., Blume, A., and Mandecki, W. (1998) *Oncogene* **16,** 1993–1999